Border Tissue Morphology Is Spatially Associated with Focal Lamina Cribrosa Defect and Deep-Layer Microvasculature Dropout in Open-Angle Glaucoma

JONG CHUL HAN, JAE HWAN CHOI, DO YOUNG PARK, EUN JUNG LEE, AND CHANGWON KEE

• PURPOSE: To investigate the topographic relationship among focal lamina cribrosa (LC) defect, microvasculature dropout (MvD) and border tissue morphology in open angle glaucoma (OAG) eyes using spectral-domain (SD) optical coherence tomography (OCT) and OCT angiography.

• DESIGN: Cross-sectional study.

• METHODS: One hundred twenty-six OAG eyes and 97 normal eyes were included. The maximum externally oblique border tissue (EOBT) length was measured by using enhanced depth imaging SD-OCT as well as focal LC defect size. Circumferential MvD width and height ratio were measured using OCT angiography.

• RESULTS: Significant correlations were found among the locations of focal LC defect, MvD and maximum EOBT length. The mean absolute locational difference was 29.1° (95% CI, −47.6 to 105.7) between focal LC defect and MvD, 10.0° (95% CI, −79.4 to 99.4) between focal LC defect and maximum EOBT length, and 10.6° (95% CI, −71.1 to 92.3) between MvD and maximum EOBT length. In multivariate logistic regression analysis, a worse VF defect was significantly associated with the presence of focal LC defects and MvDs ($P < .002$; $P = .002$, respectively). MvD circumferential width was associated with glaucoma severity ($R = -0.66$, $P < .001$), whereas focal LC defect size and MvD height ratio were associated with maximum EOBT length ($R = 0.48$, $P < .001$; $R = 0.65$, $P < .001$, respectively) and AL ($R = 0.53$, $P < .001$; $R = 0.52$, $P < .001$, respectively).

• CONCLUSIONS: There was a topographical correlation among the locations of focal LC defect, MvD and maximum border length. In addition, the presence of focal LC defect and MvD were also strongly associated with glaucoma severity. Thus, it is thought that focal LC defect and MvD may be biomarkers that reflect glaucoma severity especially at the location of maximum border tissue elongation. (Am J Ophthalmol 2019;203:89–102.

THE OPTIC NERVE HEAD (ONH) IS A KEY STRUCTURE IN glaucoma pathogenesis.[1] Glaucomatous ONH has characteristic features such as optic disc notching and thinning, and consistent retinal nerve fiber layer (RNFL) defect and a visual field (VF) defect pattern.[2,3] In addition, glaucomatous features such as RNFL defects and disc hemorrhages are usually found first in the inferotemporal area and then in the superotemporal area.[3–5] Quigley and associates[6] showed that larger lamina cribrosa (LC) pores in the inferotemporal and superotemporal areas may be why regional differences in vulnerability exist under the same intraocular pressure (IOP) in the same eye,[6] but there is no clear explanation for this to date.

Advances in imaging devices such as optical coherence tomography (OCT) have allowed detailed visualization of deep ONH structural characteristics including border tissue and Bruch's membrane. In a previous study, various border tissue shapes were observed in different ONH regions.[7] Border tissues were obliquely located internally or externally at the ONH margin. Furthermore, in glaucomatous eyes, an externally oblique border feature was usually found in the inferotemporal ONH area.[7] A recent cohort study proved that, with axial elongation, internally oblique border tissue changed into externally oblique border tissue with border tissue elongation and sometimes into γ-zone parapapillary atrophy (PPA).[8] Thus, it is likely that axial elongation accompanies border tissue elongation. Recent studies by the present authors found that the location of maximum externally oblique border tissue (EOBT) length was consistent with RNFL defect location in myopic open-angle glaucoma (OAG)[9] and also VF defect location in OAG.[10]

The focal LC defect is known to be associated with glaucoma. The presence of a focal LC defect is also associated with glaucoma severity.[11] It was frequently found in the inferotemporal area in glaucomatous eyes.[12–14] OCT angiography revealed microvasculature dropout (MvD) in border tissue and parapapillary choroid in glaucomatous

AJO.com Supplemental Material available at AJO.com.
Accepted for publication Feb 13, 2019.

Department of Ophthalmology (J.C.H., J.H.C., D.Y.P., E.J.L., C.K.), Samsung Medical Center, Sungkyunkwan University School of Medicine, Seoul, Korea.

Inquiries to Changwon Kee, Department of Ophthalmology, Samsung Medical Center, Sungkyunkwan University School of Medicine, 81 Irwon-ro, Gangnam-gu, Seoul 135-710, Korea; e-mails: cw.kee@samsung.com; ckee@skku.edu

0002-9394/$36.00
https://doi.org/10.1016/j.ajo.2019.02.023

eyes.[15,16] MvD was not only associated with glaucoma severity[17–19] it was also located in the inferotemporal ONH area in OAG eyes.[15,17,20] Interestingly, focal LC defect location was topographically associated with MvD location.[17] Additionally, focal LC defect and MvD were associated with PPA in glaucomatous eyes. The presence of focal LC defect was associated with larger PPA[21,22] and focal LC defects usually located at the maximum PPA direction in glaucomatous eyes with myopia.[21] MvD was also associated with PPA in glaucomatous eyes.[15,17,23] MvD was usually found within the PPA area in the direction of glaucomatous RNFL or VF defects.[18,19] Therefore, the present authors hypothesized that both focal LC defects and MvD may be influenced by underlying ONH shape, such as border tissue configuration with axial elongation.

To prove this hypothesis, it was first determined whether there was a topographic relationship among border tissue shape, focal LC defect, and MvD in OAG eyes. Second, the presence, size, and number of focal LC defects and MvD were addressed to identify whether they were associated with glaucoma severity, axial length (AL), and maximum EOBT length in OAG eyes. In determining MvD size, MvD circumferential width and height were measured separately.

METHODS

THIS STUDY WAS CROSS-SECTIONAL, AND SUBJECTS consisted of patients with OAG and normal controls who visited Samsung Medical Center (Seoul, South Korea) for their first ophthalmic examination, between January 2017 and December 2017. This study followed all guidelines for experimental investigation in human subjects, was approved by the Samsung Medical Center Institutional Review Board, and adhered to the tenets of the Declaration of Helsinki.

Each participant underwent a comprehensive ophthalmic examination, including slit-lamp biomicroscopy, Goldmann applanation tonometry, manifest refraction, gonioscopic examination, dilated stereoscopic examination of the ONH, color and red-free fundus photography (TRC-50DX model; Topcon Medical System, Inc., Oakland, New Jersey, USA), automated perimetry using a central 30-2 Humphrey field analyzer (HFA model 640; Humphrey Instruments, Inc., San Leandro, California, USA) with the Swedish interactive threshold algorithm standard, AL measurement (intraocular lens master; Carl Zeiss Meditec, Jena, Germany), and ultrasonographic pachymetry (Tomey SP-3000; Tomey Ltd., Nagoya, Japan). The extent of the VF defect was measured using mean deviation and pattern standard deviation. Reliable VF analysis was defined as a false-negative rate of <15%, a false-positive rate of <15%, and a fixation loss of <20%. IOPs were measured at the first and second visits without IOP-lowering medications, and average IOP values were used in the analysis.

The following criteria were required for the diagnosis of OAG. First, the presence of glaucomatous optic disc changes, such as increased cupping (vertical cup-to-disc ratio >0.7), diffuse or focal neural rim thinning; disc hemorrhage, or RNFL defects at the time of diagnosis, including second glaucomatous VF defects positive by more than 1 reliable test for at least 2 of the following 3 criteria: (1) a cluster of 3 points with a probability less than 5% on the pattern deviation map in at least 1 hemifield, including at least 1 point with a probability less than 1% or a cluster of 2 points with a probability less than 1%; (2) a glaucoma hemifield test result outside normal limits; or (3) a pattern standard deviation of 95% outside the normal limits: third, an open angle on gonioscopic examination confirmed to have no identified causes of secondary glaucoma present. To determine the dominant location of involvement, superior and inferior average hemifield values were calculated (26 points in each hemifield) in a pattern deviation plot. When 1 hemifield had a greater absolute value, it was regarded as the dominant VF defect location. Glaucoma severity was arbitrarily divided into very-early, indicating a mean deviation of more than −2 dB; early, −6 dB, less than mean deviation of ≤−2 dB; moderate, −12 dB < mean deviation of ≤−6 dB; and severe, mean deviation of ≤−12 dB. OAG with a severe VF defect was regarded as advanced glaucoma. If the patient had OAG in both eyes, one eye was randomly selected for assessment. If the patient had OAG in one eye, then the patient was assigned to one of the OAG groups, and the affected glaucoma eye was used for the assessment.

Normal eyes with open angles on gonioscopic examination and without glaucomatous optic disc or VF changes and with an IOP ≤21 mm Hg were used as normal control subjects. Normal control subjects were selected from the participants who had normal features in both eyes, and one eye was randomly selected for use in the analysis.

Exclusion criteria included eyes with medium opacities, such as a corneal or vitreous opacity, cataract, and systemic disease or ocular diseases that could affect VF test results. Eyes with mean deviation less than −25 dB and AL >30 mm were also excluded.

• **MEASUREMENT OF FOCAL LAMINA CRIBROSA DEFECTS AND MAXIMUM EXTERNALLY OBLIQUE BORDER TISSUE LENGTH:** Enhanced depth imaging (EDI) spectral-domain OCT (Heidelberg Engineering, Heidelberg, Germany) with built-in software was used to investigate focal LC defect and to measure maximum EOBT length. The value of corneal curvature was entered into the OCT system before EDI scanning to remove magnification error. Scans were performed in automatic real-time mode, which uses multiple line acquisition to reduce noise. EDI scans were obtained using 48 radial-line B-scans (each at an

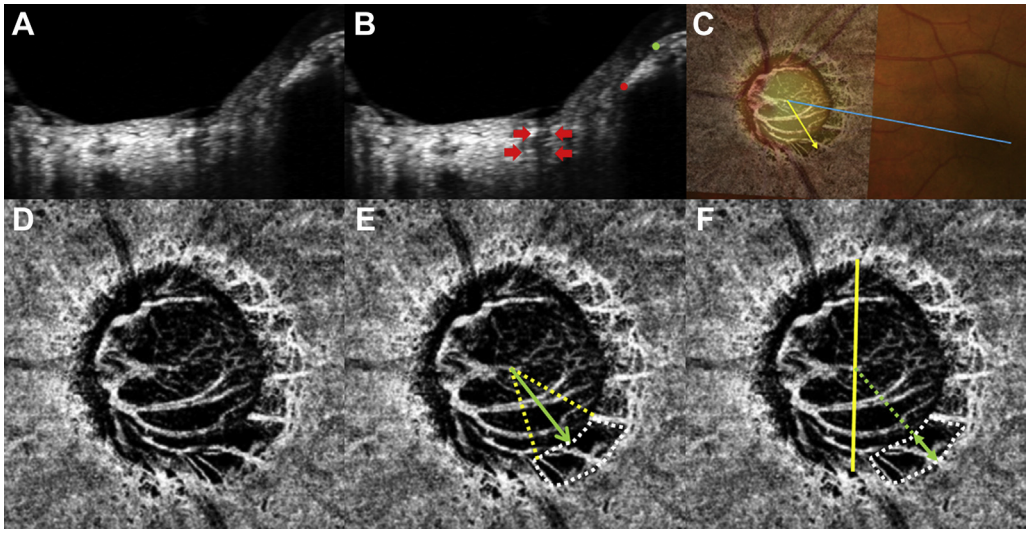

FIGURE 1. Measurement of a focal lamina cribrosa (LC) defect, a microvasculature dropout (MvD), and an externally oblique border tissue (EOBT) length. (A and B) An EDI spectral-domain OCT scan shows deep optic nerve head structures including LC and Elschnig's border tissue. Border tissue length was defined as the length between Bruch's membrane opening (BMO) (green dot) and the inner endpoint of border tissue (red dot). A focal LC defect is observed in the peripheral LC region (red arrow). (C) The angular location of the parameters was measured using the fovea-BMO axis connecting the fovea and the center of BMO (blue line). If the parameter was located below the fovea-BMO axis, it was regarded as inferior (yellow arrow). Otherwise, it was regarded as superior. (D and E) OCT angiography offers en-face images of the deep layer extending from the retinal pigment epithelium to 390 μm below Bruch's membrane that included the full thickness of the choroid and inner scleral surface. MvD located near the maximum EOBT location (white dotted area). A line connecting the center of the ONH and each endpoint of the inner margin of MvD was drawn to measure the circumferential width of MvD (yellow dotted line). The angle between the lines was defined as the circumferential width of MvD and the midpoint was used as the MvD location (green arrow). (F) MvD height was defined as the distance between the proximal and distal points of the MvD margin. We used MvD height ratio (MvD height and longest ONH line [yellow line]) to avoid ocular magnification effect.

angle of 3.75 degrees) centered on the optic disc. Each EDI scan included an average of 20 OCT frames; every other section (24 radial EDI scans in total) was selected, as previously reported.[9] OCT machine scaling was adjusted to 1:1 μm before measurement. If the scan section contained a poor quality OCT image that did not offer interpretable information with respect to Bruch's membrane opening (BMO), border tissue and LC margin due to prelaminar tissue, or overlying vessels, the next image was used. An unrecognizable image was defined as an image with <70% of the anterior LC visible or invisible border tissue morphology due to prelaminar tissue, retinal pigment epithelium, or overlying vessels. If more than 3 of 24 radial scans were unrecognizable, the eye was excluded.

Focal LC defect was defined as an anterior lamina surface irregularity violating the normal smooth curvilinear U- or W-shaped contour.[11,12,21] To avoid false positives, true defects were required to have had a maximal diameter >100 μm and a depth >30 μm; and they must also have been present in 2 neighboring radial line scans.[11,12,21] Size criteria were established in previous studies to avoid false-positive detection of a focal LC defect.[11,12] The size of the LC defect was based on imaging demonstrating the maximal length of the anterior LC defect surface. The line connecting the center of the BMO and the fovea was defined as the fovea-BMO axis. The angular location from the fovea-BMO axis was regarded as the focal LC defect location. Shadows were differentiated from LC defects by characterizing them as signal voids behind the vessels and tissues. LC defect margins were independent of the location of vessels and neural tissues.[21]

A previous study by the current group defined parameters reflecting deep ONH structures including BMO or border tissue and demonstrated that these parameters were correlated with AL.[9] Briefly, EOBT length was defined as the length between the inner end point of the EOBT tissue and the BMO.[9] In the event the border tissue had overhanging BM morphology,[7] the EOBT was only established when the inner end point of the EOBT tissue was located more internally than the BMO.

• **MEASUREMENT OF DEEP-LAYER MICROVASCULATURE DROPOUT:** The optic nerve and parapapillary area were imaged using a commercially available swept-source OCT angiography device (DRI OCT Triton, Topcon) with a central wavelength of 1,050 nm, an acquisition speed of 100,000 A-scans per second, and axial and transversal resolutions of 7 and 20 μm in tissue, respectively. Scans were

TABLE 1. Baseline Characteristics of Open-Angle Glaucoma and Normal Controls

Parameters	Open-Angle Glaucoma (N = 126)	Normal Controls (N = 97)	*P* Value
Age (y)	51.2 ± 15.4 (21-79)	55.1 ± 14.3 (20-80)	.057[a]
Males	78 (61.9)	59 (60.8)	.870[b]
Hypertension	31 (24.6)	25 (25.8)	.842[b]
Diabetes mellitus	13 (10.3)	10 (10.3)	.998[b]
Intraocular pressure (mm Hg)	17.2 ± 4.8 (9-36)	15.7 ± 3.1 (9-21)	**.005**[a]
Central corneal thickness (μm)	543.7 ± 36.5 (411-648)	550.6 ± 34.9 (462-630)	.154[a]
Axial length (mm)	25.5 ± 1.8 (22.4–29.3)	24.7 ± 1.8 (21.5–29.2)	**.002**[a]
Visual Field Parameters			
Mean deviation (dB)	−6.8 ± 6.3 (−24.5 to −1.0)	−1.4 ± 2.1 (−6.4 to 2.4)	**< .001**[a]
Pattern standard deviation (dB)	7.4 ± 4.6 (1.3–17.7)	2.8 ± 1.7 (1.2–9.6)	**< .001**[a]
Superiorly dominant field defect	92 (73.0)	-	
Advanced glaucoma	20 (15.8)	-	
Focal lamina cribrosa defect			
Presence of LC defect	54 (42.9)	21 (21.6)	**.001**[b]
Location of focal LC defect (°)	9.4 ± 39.2 (−76.9 to 77.5)	7.6 ± 35.6 (−53.1 to 75.6)	.850[a]
Inferior/superior location of focal LC defect	37 (68.5)/17 (31.5)	13 (61.9)/8 (38.1)	.584[b]
Multiple LC defect cases	16 (12.7)	1 (1.0)	.001[b]
Microvasculature dropout			
Presence of MvD	55 (43.7)	0	**< .001**[b]
Location of MvD (°)	39.9 ± 36.5 (−74.2 to 82.3)		
Inferior/superior location of MvD	47/8 (85.5/14.5)	-	
Multiple MvDs	8 (6.3)	-	
Deep optic nerve head parameters			
Presence of EOBT	92 (73.0)	63 (64.9)	.195[b]
Location of maximum EOBT length (°)	24.2 ± 34.8 (−63.8 to 87.4)	15.5 ± 42.3 (−65.6 to 82.5)	.177[a]
Inferior/superior location of maximum EOBT length	71/21 (77.2/22.8)	37/26 (58.7/41.3)	**.020**[b]

EOBT = externally oblique border tissue; LC = lamina cribrosa; MvD = microvascular dropout.
Data are mean ± standard deviation (range) or n (%), unless otherwise indicated.
Factors with statistical significance are shown in bold.
[a]Independent *t* test or Mann-Whitney *U* test.
[b]Chi-square test or Fisher exact test.

taken from 4.5- × 4.5-mm cubes, with each cube consisting of 320 × 320 pixels, with an averaging function of 4 B-scans per cube line centered on the optic disc.

Deep-layer microvasculature in the peripapillary area was evaluated on the en-face images of the peripapillary deep layer generated on the basis of the automated layer segmentation performed using OCT instrument software. The en-face images of the deep layer were derived from en-face images extending from the retinal pigment epithelium to 390 μm below Bruch's membrane that included the full thickness of the choroid and inner scleral surface. The MvD was noted when the circumferential width of the area with capillary dropout appeared more than 2× greater than the width of visible juxtapapillary microvessels with its border adjoining the optic disc margin.[18] The width and height of each MvD were measured separately, using ImageJ software (National Institutes of Health, Bethesda, Maryland, USA). To measure the circumferential width of the MvD, a line was drawn connecting the ONH center and each endpoint of the inner margin of the MvD. The angle between the lines was defined as the circumferential width of MvD. The angular location of the midpoint of the MvD circumferential width from the fovea-BMO axis was used as the MvD location. To measure MvD height, a line was drawn from the disc center to the most distal point of the MvD margin. The point at which the line met the inner MvD margin was defined as the proximal point of the MvD. The distance between the proximal and distal MvD points was defined as the MvD height (Figure 1). Because the MvD height could be affected by ocular magnification based on AL, the longest ONH axis was measured and used as the MvD height-to-length of longest axis ratio. All OCT B-scan images were required to have an image quality score ≥30 according to the manufacturer's recommendations. When the images were poor, the eyes were excluded from analysis.

• **DEFINITION OF MULTIPLE FOCAL LAMINA CRIBROSA DEFECT AND DEEP-LAYER MICROVASCULATURE DROPOUT:** The locations of focal LC defects, MvDs, and

maximum EOBT lengths were translated into a binary classifier. If the focal LC defects, MvDs, and maximum EOBT lengths were located below the fovea-BMO axis, the location was regarded as inferior. Otherwise, the location of the parameter was classified as superior. If multiple focal LC defects or MvDs existed, the location of the larger focal LC defect or MvD circumferential width was used.

Two independent observers (J.C.H. and J.H.C.), masked to the study participants' clinical information, reviewed the images to determine the presence of focal LC defects, MvDs, and EOBTs. Discrepancies were resolved by consensus. The two investigators (J.C.H. and J.H.C.) measured the size and determined the location of the parameters independently, and the averaged values determined by the 2 investigators were used in the final analysis.

• **DATA ANALYSIS:** The independent *t*-test or Mann-Whitney *U* test was used for continuous variables, and the chi-square test or Fisher exact test was used for categorical variables. Levene's test for equality of variances was also performed. Interobserver agreement in terms of the presence of focal LC defect and the determination of EOBT and MvD was evaluated by the calculation of κ coefficients. The interobserver reproducibility of the size and location of focal LC defect, MvD, and maximum EOBT length was assessed by calculating the intraclass correlation coefficient.

Fisher's exact test and the κ test were used to evaluate location correspondence among the parameters (focal LC defect, MvD, dominant VF defect, and maximum EOBT length). ANOVA test and Tukey post hoc analyses were used to compare the parameters according to VF defect severity or the presence of MvD and a focal LC defect. Pearson's correlation was used to assess correlations among continuous variables, and the correlation coefficient (*R*) was calculated. The Bland-Altman method was used to show the means relative to differences among the variables.

Univariate and multivariate logistic regression analyses were performed to identify factors associated with the presence of MvD and focal LC defect. Factors with a *P* value of <.2 on univariate analysis were included in the multivariate analysis. However, because the presence of an LC defect was correlated with MvD, these variables were included in 2 separate multivariate analysis model.

RESULTS

THE PRESENT STUDY INCLUDED 167 OAG EYES FROM 167 PATIENTS with OAG and 112 participants with normal eyes. Among these eyes, 41 OAG eyes (24.6%) and 15 normal eyes (13.4%) were excluded because they had poor image quality (24 OAG eyes and 11 normal eyes), unreliable VF

TABLE 2. Interobserver Agreement and Reproducibility in Measurement of Parameters

Presence of Parameters	Kappa Value (95% CI)	Location of Parameters	ICC Value (95% CI)	Extent of Parameters	ICC Value (95% CI)
EOBT	0.916 (0.887–0.945)	Maximum EOBT length (°)	0.958 (0.942–0.970)	Maximum EOBT length (μm)	0.972 (0.962–0.980)
Lamina cribrosa defect	0.778 (0.734–0.822)	Lamina cribrosa defect (°)	0.944 (0.912–0.964)	Lamina cribrosa defect size (μm)	0.908 (0.858–0.941)
Microvasculature dropout	0.809 (0.766–0.852)	Microvasculature dropout (°)	0.956 (0.926–0.974)	Microvasculature dropout width (°)	0.987 (0.977–0.992)
				Microvasculature dropout height ratio	0.965 (0.940–0.979)

CI = confidence interval; EOBT = externally oblique border tissue; ICC = intraclass correlation.

TABLE 3. Relationships Among the Locations of Dominant Visual Field Defect, Focal Lamina Cribrosa Defect, and Microvasculature Dropout

Dominant Visual Field Defect Location	Lamina Cribrosa Defect Location (n = 54)			Microvascular Dropout Location (n = 55)			Microvasculature dropout location	Lamina Cribrosa Defect Location (n = 35)		
	Inferior	Superior	Total	Inferior	Superior	Total		Inferior	Superior	
Inferior	31	9	40	41	4	45	Inferior	23	5	28
Superior	6	8	14	6	4	10	Superior	1	6	7
Total	37	17	54	47	8	55		24	11	35
	$P = .023$, $\kappa = 0.32$, confidence interval, 0.18–0.46			$P = .029$, $\kappa = 0.34$, confidence interval, 0.17–0.50				$P = .002$, $\kappa = 0.56$, confidence interval, 0.41–0.71		

TABLE 4. Locations of Maximum Externally Oblique Border Tissue Length Versus Microvascular Dropout and Focal Lamina Cribrosa Defect

Maximum Externally Oblique Border Tissue Length Location	Lamina Cribrosa Defect Location (n = 47)			Microvascular Dropout Location (n = 49)		
	Inferior	Superior	Total	Inferior	Superior	Total
Inferior	28	6	34	38	3	41
Superior	6	7	13	5	3	8
Total	34	13	47	43	6	49
	$P = .026$ $\kappa = 0.36$, confidence interval, 0.21–0.51			$P = .047$, $\kappa = 0.34$, confidence interval, 0.15–0.52		

test results (9 OAG eyes and 3 normal eyes), advanced glaucoma with mean deviation less than −25 dB (6 OAG eyes), and myopia with AL >30 mm (2 OAG eyes and 1 normal eye). A total of 126 OAG eyes and 97 normal eyes were included in the analysis. There were no significant differences in age, sex, history of hypertension, history of diabetes, or central corneal thickness between the OAG eyes and the normal eyes. However, OAG eyes demonstrated higher IOP and longer AL than those of normal control subjects ($P = .005$ and $P = .002$, respectively). VF global indexes, mean deviation, and pattern standard deviations were significantly different between OAG eyes and normal control eyes ($P < .001$ for both parameters). Among OAG eyes, 92 eyes (73.0%) had superior dominant field defects, and 20 eyes (15.8%) demonstrated advanced stage glaucoma. OAG eyes had a significantly higher prevalence of LC defects (42.9% vs. 21.6%) and multiple LC defects (12.7% vs. 1.0%) than normal eyes ($P < .001$ for both parameters). The inferior-to-superior ratios of focal LC defects were not significantly different between the OAG and the normal eyes. The MvD was found in 55 OAG eyes (43.7%), and multiple MvDs were found in 8 OAG eyes (6.3%). Among OAG eyes with MvDs, the MvDs were found in inferior locations in 47 eyes (85.5%). Meanwhile, no MvD was found in normal eyes. EOBT was found in at least 1 section in 92 OAG eyes (73.0%) and in 63 normal eyes (64.9%). Maximum EOBT locations were found more frequently in inferior locations in OAG eyes than in normal eyes ($P = .02$) (Table 1).

Interobserver agreement was moderate to strong in terms of the presence of each parameter (0.778–0.916). Interobserver reproducibility of the location and the extent of the parameters was excellent (0.908–0.987) (Table 2).

When the 54 OAG eyes with presence of the focal LC defect were analyzed, there was a topographical correlation between the locations of the focal LC defect and the dominant VF defect ($\kappa = 0.32$; 95% confidence interval [CI], 0.18–0.46; $P = .023$). Among the 55 OAG eyes with MvD, there was a topographical correlation between the locations of the MvD and dominant VF defects ($\kappa = 0.34$; 95% confidence interval [CI], 0.17–0.50; $P = .029$). When the 35 OAG eyes affected with both the MvD and the focal LC defect were analyzed, the MvD was topographically associated with the focal LC defect ($\kappa = 0.56$; 95% CI, 0.41–0.71; $P = .002$) (Table 3). Among the 47 OAG eyes with both EOBT and focal LC defects, focal LC defect locations were topographically associated with the location of maximum EOBT length ($\kappa = 0.36$; 95% CI, 0.21–0.51; $P = .026$). When the 49 OAG eyes with both EOBT and MvD were analyzed, MvD location was consistent with the location of maximum EOBT length ($\kappa = 0.34$; 95% CI, 0.15–0.52; $P = .047$) (Table 4).

Pearson's correlation analysis showed that focal LC defect location was significantly correlated with MvD location ($R = 0.62$; $P < .001$). Focal LC defect location

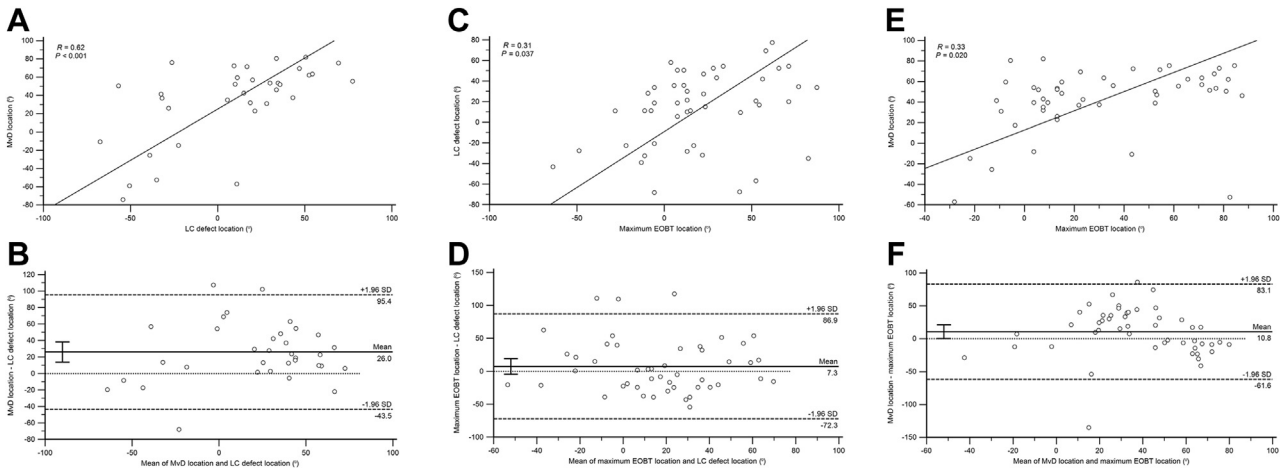

FIGURE 2. Correlation and agreement among the parameters. In Pearson's correlation analysis, the focal lamina cribrosa (LC) defect location was significantly correlated with microvasculature dropout (MvD) location (E) and location of the maximum externally oblique border tissue (EOBT) length (C). MvD location was also significantly correlated with the maximum EOBT length location (A). Bland-Altman plot shows the mean difference between each parameter with the limits of agreement (B, D, F).

TABLE 5. Correlation Analysis Among the Parameters in Open-Angle Glaucoma Patients With Microvasculature Dropout or Focal Lamina Cribrosa Defect

Parameters	MvD Circumferential Width (°)	MvD Height Ratio	Focal LC Defect Size (μm)
Mean deviation of VF (dB)			
Pearson coefficient	−0.66	−0.02	−0.10
P value[a]	**< .001**	.869	.457
Maximum EOBT length (μm)			
Pearson coefficient	−0.14	0.65	0.48
P value[a]	.308	**< .001**	**< .001**
Axial length (mm)			
Pearson coefficient	−0.08	0.52	0.53
P value[a]	.556	**< .001**	**< .001**

EOBT = externally oblique border tissue; LC = lamina cribrosa; MvD = microvasculature dropout; VF = visual field.
[a]Factors with statistical significance are shown in bold.

was also significantly correlated with maximum EOBT location ($R = 0.31$; $P = .037$). MvD location was significantly correlated with maximum EOBT length location ($R = 0.33$; $P = .020$). Bland-Altman plots showed that the mean difference was 26.0 (95% CI, −43.5 to 95.4) between focal LC defect location and MvD location, 7.3 (95% CI, −72.3 to 86.9) between focal LC defect location and maximum EOBT location, and 10.8 (95% CI, −61.1 to 83.1) between MvD location and maximum EOBT location (Figure2). The mean deviation value of the VF defect was significantly correlated with MvD circumferential width but not with MvD height ratio or focal LC defect size. Meanwhile, maximum EOBT length and AL were significantly correlated with MvD height ratio and focal LC defect size but not with MvD circumferential width (Table 5).

When OAG eyes were divided into 4 groups according to mean deviation values, no significant differences were found in regard to age, IOP, central corneal thickness, AL, or the presence of EOBT among the groups. However, focal LC defect and MvD were found more frequently with worse mean deviation severity ($P = .006$ and $P < .001$, respectively). Multiple MvDs were found more frequently with worse mean deviation severity ($P = .002$) (Table 6). When OAG eyes were divided into 4 groups according to the presence of MvD and focal LC defect, the OAG eyes with MvD showed greater glaucoma severity than the other groups regardless of the presence of a focal LC defect

TABLE 6. Comparisons of Parameters According to Visual Field Defect Severity in Open-Angle Glaucoma

	Very Early (MD > −2dB) (n = 36)	Early (−6dB< MD≤ −2dB) (n = 39)	Moderate (−12dB< MD≤ −6dB) (n =31)	Advanced (MD ≤ −12dB) (n =20)	*P* Value
Mean deviation (dB)	−1.4 ± 0.3 (−2.0 to −1.0)	−3.9 ± 1.0 (−5.8 to −2.1)	−8.5 ± 1.6 (−11.7 to −6.0)	−19.2 ± 4.4 (−24.5 to −12.0)	**<.001**[a]
Age (y)	49.7 ± 12.2 (21-72)	51.2 ± 15.0 (22-77)	51.5 ± 16.8 (25-79)	54.2 ± 18.7 (21-76)	.773[a]
Intraocular pressure (mm Hg)	17.1 ± 4.5 (12-32)	16.5 ± 3.9 (10-32)	16.6 ± 4.7 (9-28)	19.6 ± 6.2 (11-36)	.086[a]
Central corneal thickness (μm)	544.3 ± 28.2 (471-604)	538.8 ± 32.5 (486-629)	552.9 ± 37.5 (472-632)	537.6 ± 52.2 (411-648)	.357[a]
Axial length (mm)	25.2 ± 1.3 (22.6–28.1)	25.3 ± 1.8 (22.5–29.2)	25.8 ± 2.1 (22.5–29.3)	26.0 ± 2.0 (22.9–29.3)	.272[a]
Presence of focal LC defect	9 (25.0)	14 (35.9)	18 (58.1)	13 (65.0)	**.006**[b]
Multiple focal LC defect	2 (5.6)	5 (12.8)	5 (16.1)	4 (20.0)	.400[b]
Presence of MvD	1 (2.8)	13 (33.3)	23 (74.2)	18 (90.0)	**<.001**[b]
Multiple MvD	0	2 (5.1)	4 (12.9)	6 (30.0)	**.002**[b]
Presence of EOBT	26 (72.2)	25 (64.1)	25 (80.6)	16 (80.0)	.392[b]

EOBT = externally oblique border tissue; LC = lamina cribrosa; MvD = microvascular dropout.
Factors with statistical significance are shown in bold.
Data are mean ± standard deviation (range) or n (%) unless otherwise indicated.
[a]ANOVA test.
[b]Chi-square test or Fisher exact test.

(*P* < .001). EOBT was found more frequently in OAG eyes with a focal LC defect alone, with MvD alone and both the focal LC defects, and with MvD than OAG eyes without a focal LC defect and MvD (*P* = .001) (Table 7).

Logistic regression showed that more severe mean deviation, presence of the focal LC defect, and greater EOBT length were significantly associated with MvD in OAG eyes on univariate and multivariate analyses (Table 8). More severe mean deviation, presence of MvD, and greater EOBT length were significantly associated with the presence of focal LC defects on univariate and multivariate analyses (Table 9).

DISCUSSION

THE PRESENT STUDY HAS SEVERAL SIGNIFICANT FINDINGS. First, the maximum border tissue elongation was topographically associated with focal LC defect and the MvD locations. The MvD location was associated with the focal LC defect location as in previous reports.[17] In addition, both the focal LC defects and the MvDs were usually found near the location of maximum EOBT length in OAG eyes. Second, glaucoma severity was significantly associated with the presence of MvD and focal LC defects. The presence of the MvD was more strongly associated with greater glaucoma severity than the presence of the focal LC defect. Furthermore, the MvD was not found even in 1 normal eye, whereas the focal LC defect was found in a few cases. Third, MvD circumferential width was significantly correlated with glaucoma severity; however, focal LC defect size and MvD height ratio were significantly correlated with AL and maximum EOBT length (Figure 3).

ONH deep structures consist of various features of border tissue and Bruch's membrane according to ONH region.[7] A recent cohort study demonstrated that border tissue could be externally elongated and located closer to the ONH surface with axial growth.[8] Furthermore, some myopic eyes demonstrated border tissue changes with axial growth, although they did not show ONH surface changes.[8] A recent study conducted by the present authors showed that deep ONH morphology, such as border length, was associated with a VF pattern even in OAG eyes with round ONH surface margins.[10] It seems that deep ONH shape sometimes offers more information about regional ONH morphological differences than the ONH surface.

The present study showed that border tissue morphology may be significantly associated with focal LC defect and MvD location. The focal LC defect was topographically associated with the MvD as previously reported.[17] These 2 factors were also topographically associated with maximum EOBT length, that is, the

TABLE 7. Comparisons of Parameters According to Presence of Microvascular Dropout and Lamina Cribrosa Defects in Open-Angle Glaucoma

	MvD (+) only (A) (n = 20)	LC defect (+) & MvD (+) (B) (n = 35)	LC defect (+) only (C) (n = 19)	LC defect (–) & MvD (–) (D) (n = 52)	*P* Value	Post Hoc Analysis
Age (y)	54.6 ± 16.3 (22-77)	50.7 ± 16.8 (24-78)	48.2 ± 11.8 (31-69)	51.5 ± 15.1 (21-79)	.620[a]	
Intraocular pressure (mm Hg)	17.6 ± 6.0 (11-36)	16.9 ± 4.4 (9-27)	16.4 ± 4.9 (11-32)	17.4 ± 4.5 (11-32)	.807[a]	
Central corneal thickness (μm)	539.6 ± 40.7 (483-618)	546.8 ± 43.7 (411-648)	541.3 ± 34.1 (471-629)	544.0 ± 30.7 (472-606)	.898[a]	
Axial length (mm)	25.3 ± 2.2 (22.8–29.2)	26.1 ± 1.9 (22.9–29.3)	25.1 ± 1.6 (22.6–28.1)	25.3 ± 1.6 (22.5–29.3)	.133[a]	
Mean deviation (dB)	−8.9 ± 5.8 (−24.2 to −1.2)	−12.1 ± 7.1 (−24.5 to −2.6)	−3.3 ± 2.3 (−8.8 to −1.1)	−3.7 ± 3.9 (−22.9 to −1.0)	**< .001**[a]	**A = B > C = D**
Presence of EOBT	17 (85.0)	32 (91.4)	15 (78.9)	28 (53.8)	**.001**[b]	
Maximum EOBT length (μm)	367.7 ± 429.3 (117-1912)	493.7 ± 337.3 (122-1,250)	483.1 ± 308.9 (115-1,118)	437.9 ± 233.3 (102-1,197)	.603	
MvD circumferential width (°)	25.7 ± 14.7 (5.4–46.0)	38.8 ± 36.9 (7.1–139.0)	-	-	.070[c]	
MvD height ratio	0.2 ± 0.1 (0.1–0.6)	0.2 ± 0.1 (0.1–0.6)	-	-	.911[c]	
Focal LC defect size (μm)	-	130.4 ± 43.9 (100-267)	130.6 ± 34.5 (100-242)	-	.987[c]	

EOBT = externally oblique border tissue; LC = lamina cribrosa; MvD = microvascular dropout.
Factors with statistical significance are shown in bold.
Data are mean ± standard deviation (range) or n (%) unless otherwise indicated.
[a]ANOVA test, a significant difference between the groups was shown in bold in post hoc analysis.
[b]Chi-square test or Fisher exact test.
[c]Mann-Whitney *U* test.

TABLE 8. Logistic Regression Testing Factors Associated With the Presence of Microvasculature Dropout in Open-Angle Glaucoma

	Univariate Analysis			Multivariate Analysis 1			Multivariate Analysis 2		
Parameter	OR	95% CI	*P* Value	OR	95% CI	*P* Value	OR	95% CI	*P* Value
Age (y)	1.007	0.984–1.030	.576						
Intraocular pressure (mm Hg)	1.002	0.930–1.079	.958						
Central corneal thickness (μm)	1.001	0.991–1.010	.885						
Axial length (mm)	1.171	0.959–1.428	.121	1.042	0.807–1.343	.754	0.938	0.717–1.227	.639
Mean deviation (dB)	0.714	0.626–0.815	**<.001**	0.729	0.638–0.833	**<.001**	0.691	0.596–0.801	**<.001**
Focal LC defect presence	4.789	2.239–10.243	**<.001**	3.326	1.314–8.418	**.011**			
EOBT presence	5.312	2.011–14.059	**.001**				15.366	2.935–80.443	**.001**

CI = confidence interval; EOBT = externally oblique border tissue; LC = lamina cribrosa; OR = odds ratio.
Factors with statistical significance are shown in bold.
Focal LC defect was strongly correlated with EOBT presence, thus each factor was included in the different model in multivariate analysis.

TABLE 9. Logistic Regression Testing Factors Associated with the Presence of Focal Lamina Cribrosa Defect in Open-Angle Glaucoma

	Univariate Analysis			Multivariate Analysis 1			Multivariate Analysis 2		
	OR	95% CI	*P* Value	OR	95% CI	*P* Value	OR	95% CI	*P* Value
Age (y)	0.989	0.966–1.012	.355						
Intraocular pressure (mm Hg)	0.966	0.894–1.043	.376						
Central corneal thickness (μm)	1.002	0.992–1.011	.744						
Axial length (mm)	1.142	0.937–1.393	.188	1.023	0.823–1.271	.839	1.090	0.882–1.348	.424
Mean deviation (dB)	0.901	0.844–0.961	**.002**	0.900	0.841–0.962	**.002**			
MvD presence	4.789	2.239–10.243	**<.001**				4.624	2.151–9.937	**<.001**
EOBT presence	4.029	1.595–10.173	**.003**	4.189	1.527–11.489	**.005**			

CI = confidence interval; EOBT = externally oblique border tissue; LC = lamina cribrosa; OR = odds ratio.
Factors with statistical significance are shown in bold.
MvD was strongly associated with mean deviation and EOBT presence, thus MvD was included in the different model in multivariate analysis.

relationship between focal LC defect and MvD may be explained by border tissue morphology. It has previously been shown that ONH geometric morphology is related to glaucomatous defects in glaucomatous eyes. For instance, the PPA and disc tilt are known to be topographically associated with RNFL defects in glaucomatous eyes.[24–28] The PPA and disc tilt have also been reported to be associated with focal LC defects in OAG eyes with myopia.[29] In the present authors' previous study, EDI-OCT results showed that the location of the maximum border length was consistent with the location of disinsertion type LC defect in myopic OAG eyes.[21] Furthermore, the PPA was associated with MvDs in that all MvDs were found within the PPA, including the region of parapapillary choroid or border tissue.[15,17,30] Given that focal LC defects and MvDs were found at the location of maximum border length in the present study, the authors speculated that the focal LC defect and the MvD were influenced by structural vulnerability at the location of the greatest border tissue elongation in the ONH.

In the present study, glaucoma severity was significantly associated with the presence of focal LC defect and MvD in OAG eyes. However, there were several differences between focal LC defect and MvD with regard to glaucoma severity. First, MvD was significantly associated with more severe mean deviation regardless of focal LC defects; meanwhile, focal LC defect was associated with more severe mean deviation only when there was a coexisting MvD. Furthermore, in eyes with more advanced OAG, there were more frequent instances of multiple MvDs but not multiple focal LC defects than in eyes with early stage OAG. Second, the MvD was not found in even 1 normal eye, whereas the focal LC defect was found in some normal

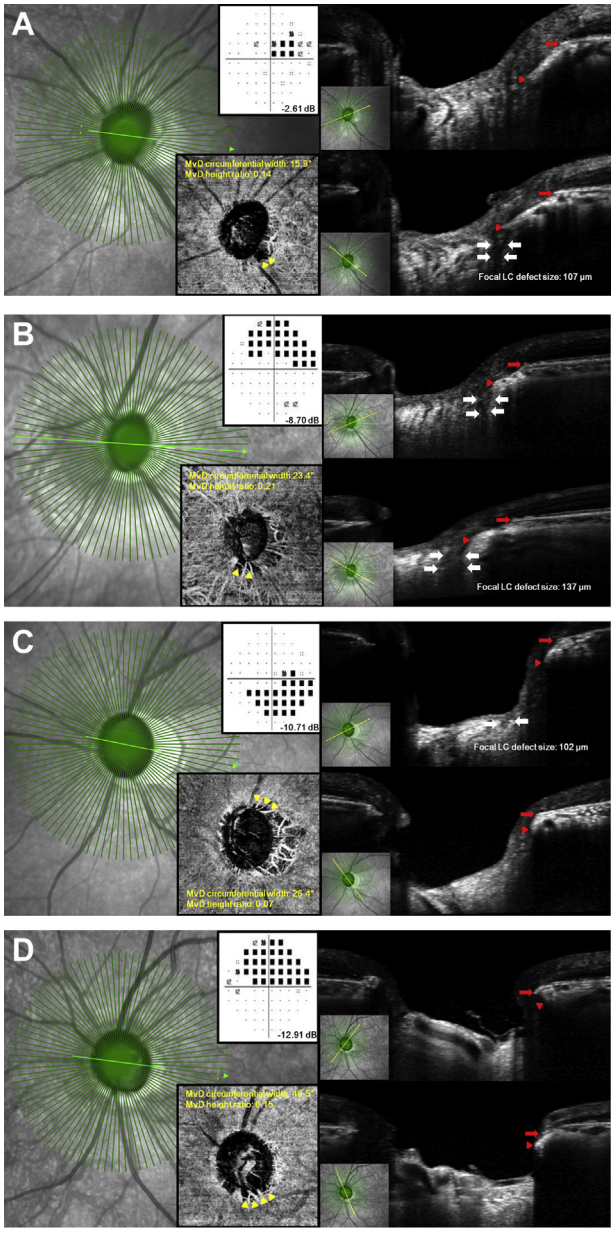

FIGURE 3. Representative cases. (A) A 40-year-old female with early stage open-angle glaucoma (OAG) (mean deviation, −2.61 dB, axial length [AL]: 25.6 mm). The length between Bruch's membrane opening (red arrow) and the inner margin of border tissue (red arrowhead) was defined as the externally oblique border tissue (EOBT) length. The maximum EOBT was located in the inferotemporal area, which was consistent with the location of the focal lamina cribrosa (LC) defect (white arrow) and microvasculature dropout (MvD) (yellow arrowhead). (B) A 68-year-old male with moderate stage OAG (mean deviation: −8.70 dB, AL: 27.2 mm). The focal LC defect was located in both inferior and superior directions (white arrow). However, the largest focal LC defect was located inferiorly, and it was consistent with the locations of maximum EOBT length and MvD (yellow arrowhead). (C) A 50-year-old male with moderate stage OAG (mean deviation: −10.71 dB, AL: 24.6 mm). The focal LC defect (white arrow) and MvD (yellow arrowheads) were located in the region of maximum EOBT length (superotemporal direction). (D) A 55-year-old female with advanced stage OAG (mean deviation: −12.91 dB, AL: 23.0 mm). MvD (arrowhead) was found at the maximum EOBT length location (inferotemporal area). Focal LC defect was not found in this eye. In all cases, there was locational correspondence among maximum EOBT length, focal LC defect, MvD, and dominant visual field defect. Among the cases, the circumferential width of MvD was largest in cases of advanced OAG eye (D) and smallest in cases of early stage OAG (A). However, MvD height ratio and focal LC defect size were greatest in the OAG eye with the largest AL (B) compared to that in other cases regardless of glaucoma severity.

controls (21.6%). In addition, MvD was found in just 1 case (2.8%) of very-early stage glaucoma. An explanation is not currently forthcoming for why there were differences in the presence of focal LC defects and MvDs according to glaucoma severity based on the current study's data; but it seems that the MvD may be associated with more advanced glaucoma than the focal LC defect in OAG eyes. As previously reported, MvD may be associated with signs of glaucomatous progression such as disc hemorrhage,[30] and therefore MvD could be found more in advanced glaucoma.

Considering the presence of focal LC defect and MvD was associated with the glaucoma severity in OAG eyes, the authors speculated that the sizes of focal LC defects and MvDs may also be associated with glaucoma severity. However, when the width and height of MvD were measured separately, only MvD circumferential width was associated with glaucoma severity, whereas focal LC defect sizes and MvD height ratios were not. Instead, focal LC defect size and MvD height ratio were associated with the extent of AL and maximum EOBT lengths. Previously, we reported that focal LC defects are associated with myopia and AL.[21] MvD height is also likely to be associated with axial elongation and stretching around ONH. Hypothetically, this phenomenon occurred because MvDs are found in the border tissue and parapapillary choroid.[18,23] In a previous study, it was shown that MvD could occur only in the border tissue area.[16] Thus, in the eyes with short ALs, it could be difficult to confirm the presence of MvD, if the border tissue is not externally oblique. Longer AL may cause border tissues to be exposed externally, leading to greater MvD height on the border tissue (Figure 4).

Biomechanically, ONH geometry and tissue information are known to be associated with glaucoma pathogenesis as well as IOP-related stress.[1,31] All these factors may contribute to glaucomatous damage under a given IOP. During the growth period, the deep and superficial ONH may change with axial elongation, and it is likely that the inferotemporal ONH area experiences the greatest morphologic changes. Consequently, the ONH structural features may undergo stresses and strains that differ from region to region under a given IOP, initially leading to

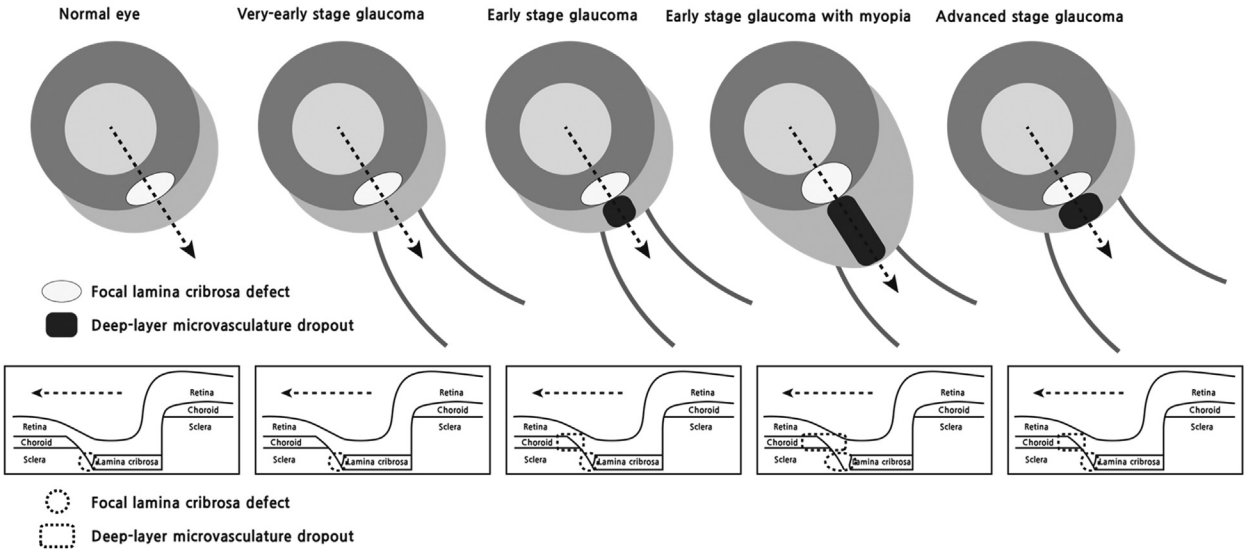

FIGURE 4. The relationships among focal lamina cribrosa (LC) defect, microvasculature dropout (MvD), and maximum externally oblique border tissue (EOBT) length in eyes with open-angle glaucoma (OAG). The maximum EOBT length was usually located inferotemporally (dotted arrow). The focal LC defect was also found at the location of maximum EOBT length. Focal LC defect was larger in eyes with larger axial length (AL) and maximum EOBT length. The MvD was also observed at the location of maximum EOBT length. The circumferential width of MvD was greater in more severe OAG. However, the height of MvD and the size of focal LC defect was greater in eyes with larger AL and maximum EOBT length. The focal LC defect (dotted circle) and MvD (dotted square) were anatomically close to each other because both were usually found at the peripheral deep region of the ONH at the location of maximum EOBT length.

retinal ganglion cell axonal damage with connective tissue remodeling at the most vulnerable location in the ONH. The locations of the focal LC defects (usually peripheral LC)[1,31] and MvDs (border tissue or parapapillary choroid)[16] are anatomically near to one another. Given that the greatest IOP-related stress usually occurs at the ONH margin, the structures in the deep ONH margin such as peripheral LC, border tissue, and parapapillary choroid may also be more vulnerable than other structures under the same IOP. As a result, the focal LC defect could form in the peripheral LC, whereas the MvD may appear in the border tissue and parapapillary choroid at the most vulnerable ONH location in OAG eyes.

The present study has some limitations, the first of which is its cross-sectional design. Mean deviation severity is referred to as the parameter reflecting the temporal progression of glaucomatous changes in this study. Causal factors usually must be identified in the earlier stages of disease. Because MvD was not found in normal eyes and even in very early stage OAG eyes, the MvD was regarded more as the factor associated with the outcome rather than the cause of glaucomatous ONH defect. However, to know the causal relationship clearly, a prospective study is warranted. Second, projection artifacts associated with superficial vessels on OCT angiography and overlying vessels and prelaminar tissue in EDI-OCT could have affected the presence and numbers of the MvD and focal LC defect. However, only MvD and focal LC defect that met the criteria were regarded as significant findings. Furthermore, there was good interobserver agreement between investigators. Regardless, interpretation of the study results should be done with consideration of the image quality-related limitations. Third, the locations were only defined using maximum values or midpoints of the width of the parameters. Because each parameter such as LC defect or MvD can have different widths even with the same location of maximum values or midpoints, the locational agreement would be different if the width was considered in the analysis. Fourth, the criteria for the minimum size of the focal LC defect and the MvD were arbitrary. There were small focal LC defects of <100 μm and MvD with partially decreased capillaries. Consideration of clinical characteristics of the eyes with these features is warranted in future work.

In conclusion, there were topographical associations among focal LC defects, MvD, and maximum border length. Considering that focal LC defects and MvD are strongly associated with the presence and severity of glaucoma, the authors hypothesize that the focal LC defect and the MvD may be the biomarkers that reflect glaucoma severity, especially at the location of maximum border tissue elongation in OAG eyes.

ALL AUTHORS HAVE COMPLETED AND SUBMITTED THE ICMJE FORM FOR DISCLOSURE OF POTENTIAL CONFLICTS OF INTEREST and none were reported. This research was supported by the Basic Science Research Program through the National Research Foundation of Korea (NRF) funded by Ministry of Education grant 2017R1D1A1B03034834. The authors have no proprietary or commercial interest in any materials discussed in this article.

REFERENCES

1. Burgoyne CF, Downs JC, Bellezza AJ, Suh JK, Hart RT. The optic nerve head as a biomechanical structure: a new paradigm for understanding the role of IOP-related stress and strain in the pathophysiology of glaucomatous optic nerve head damage. *Prog Retin Eye Res* 2005;24(1):39–73.
2. Jonas JB, Gusek GC, Naumann GO. Optic disc morphometry in chronic primary open-angle glaucoma. I. Morphometric intrapapillary characteristics. *Graefes Arch Clin Exp Ophthalmol* 1988;226(6):522–530.
3. Jonas JB, Fernandez MC, Sturmer J. Pattern of glaucomatous neuroretinal rim loss. *Ophthalmology* 1993;100(1):63–68.
4. Garway-Heath DF, Ruben ST, Viswanathan A, Hitchings RA. Vertical cup/disc ratio in relation to optic disc size: its value in the assessment of the glaucoma suspect. *Br J Ophthalmol* 1998;82(10):1118–1124.
5. Shin DH, Lee MK, Briggs KS, Kim C, Zeiter JH, McCarty B. Intraocular pressure-related pattern of optic disc cupping in adult glaucoma patients. *Graefes Arch Clin Exp Ophthalmol* 1992;230(6):542–546.
6. Quigley HA, Addicks EM. Regional differences in the structure of the lamina cribrosa and their relation to glaucomatous optic nerve damage. *Arch Ophthalmol* 1981;99(1):137–143.
7. Reis AS, Sharpe GP, Yang H, Nicolela MT, Burgoyne CF, Chauhan BC. Optic disc margin anatomy in patients with glaucoma and normal controls with spectral domain optical coherence tomography. *Ophthalmology* 2012;119(4):738–747.
8. Kim M, Choung HK, Lee KM, Oh S, Kim SH. Longitudinal changes of optic nerve head and peripapillary structure during childhood myopia progression on OCT: Boramae myopia cohort study report 1. *Ophthalmology* 2018;125(8):1215–1223.
9. Han JC, Lee EJ, Kim SB, Kee C. The characteristics of deep optic nerve head morphology in myopic normal tension glaucoma. *Invest Ophthalmol Vis Sci* 2017;58(5):2695–2704.
10. Han JC, Choi JH, Park DY, Lee EJ, Kee C. Deep optic nerve head morphology is associated with pattern of glaucomatous visual field defect in open-angle glaucoma. *Invest Ophthalmol Vis Sci* 2018;59(10):3842–3851.
11. You JY, Park SC, Su D, Teng CC, Liebmann JM, Ritch R. Focal lamina cribrosa defects associated with glaucomatous rim thinning and acquired pits. *JAMA Ophthalmol* 2013;131(3):314–320.
12. Tatham AJ, Miki A, Weinreb RN, Zangwill LM, Medeiros FA. Defects of the lamina cribrosa in eyes with localized retinal nerve fiber layer loss. *Ophthalmology* 2014;121(1):110–118.
13. Kiumehr S, Park SC, Syril D, et al. In vivo evaluation of focal lamina cribrosa defects in glaucoma. *Arch Ophthalmol* 2012;130(5):552–559.
14. Suh MH, Zangwill LM, Manalastas PI, et al. Optical coherence tomography angiography vessel density in glaucomatous eyes with focal lamina cribrosa defects. *Ophthalmology* 2016;123(11):2309–2317.
15. Lee EJ, Lee KM, Lee SH, Kim TW. Parapapillary choroidal microvasculature dropout in glaucoma: a comparison between optical coherence tomography angiography and indocyanine green angiography. *Ophthalmology* 2017;124(8):1209–1217.
16. Lee EJ, Kim TW, Lee SH, Kim JA. Underlying microstructure of parapapillary deep layer capillary dropout identified by optical coherence tomography angiography. *Invest Ophthalmol Vis Sci* 2017;58(3):1621–1627.
17. Suh MH, Zangwill LM, Manalastas PI, et al. Deep retinal layer microvasculature dropout detected by the optical coherence tomography angiography in glaucoma. *Ophthalmology* 2016;123(12):2509–2518.
18. Lee EJ, Kim TW, Kim JA, Kim JA. Parapapillary deep layer microvasculature dropout in primary open-angle glaucoma eyes with a parapapillary gamma-zone. *Invest Ophthalmol Vis Sci* 2017;58(13):5673–5680.
19. Lee EJ, Lee SH, Kim JA, Kim TW. Parapapillary deep layer microvasculature dropout in glaucoma: topographic association with glaucomatous damage. *Invest Ophthalmol Vis Sci* 2017;58(7):3004–3010.
20. Akagi T, Iida Y, Nakanishi H, et al. Microvascular density in glaucomatous eyes with hemifield visual field defects: an optical coherence tomography angiography study. *Am J Ophthalmol* 2016;168:237–249.
21. Han JC, Cho SH, Sohn DY, Kee C. The Characteristics of lamina cribrosa defects in myopic eyes with and without open-angle glaucoma. *Invest Ophthalmol Vis Sci* 2016;57(2):486–494.
22. Kimura Y, Akagi T, Hangai M, et al. Lamina cribrosa defects and optic disc morphology in primary open angle glaucoma with high myopia. *PLoS One* 2014;9(12):e115313.
23. Lee SH, Lee EJ, Kim TW. Topographic correlation between juxtapapillary choroidal thickness and parapapillary deep layer microvasculature dropout in primary open-angle glaucoma. *Br J Ophthalmol* 2018;102(8):1134–1140.
24. Park KH, Tomita G, Liou SY, Kitazawa Y. Correlation between peripapillary atrophy and optic nerve damage in normal-tension glaucoma. *Ophthalmology* 1996;103(11):1899–1906.
25. Cho BJ, Park KH. Topographic correlation between beta-zone parapapillary atrophy and retinal nerve fiber layer defect. *Ophthalmology* 2013;120(3):528–534.
26. Park HY, Lee K, Park CK. Optic disc torsion direction predicts the location of glaucomatous damage in normal-tension glaucoma patients with myopia. *Ophthalmology* 2012;119(9):1844–1851.
27. Choi JA, Park HY, Shin HY, Park CK. Optic disc tilt direction determines the location of initial glaucomatous damage. *Invest Ophthalmol Vis Sci* 2014;55(8):4991–4998.

28. Lee KS, Lee JR, Kook MS. Optic disc torsion presenting as unilateral glaucomatous-appearing visual field defect in young myopic Korean eyes. *Ophthalmology* 2014;121(5):1013–1019.
29. Sawada Y, Araie M, Ishikawa M, Yoshitomi T. Multiple temporal lamina cribrosa defects in myopic eyes with glaucoma and their association with visual field defects. *Ophthalmology* 2017;124(11):1600–1611.
30. Park HL, Kim JW, Park CK. Choroidal microvasculature dropout is associated with progressive retinal nerve fiber layer thinning in glaucoma with disc hemorrhage. *Ophthalmology* 2018;125(7):1003–1013.
31. Yang H, Reynaud J, Lockwood H, et al. The connective tissue phenotype of glaucomatous cupping in the monkey eye: clinical and research implications. *Prog Retin Eye Res* 2017;59:1–52.